Polymer-assisted microcontact printing: Using a tailor-made polydimethylsiloxane (PDMS) stamp for precise patterning of rough surfaces

Nazim Pallab,[ab] Stefan Reinicke,[b] Johannes Gurke,[a] Rainer Rihm,[b] Sergio Kogikoski Jr.,[a] Matthias Hartlieb,[ab] and Martin Reifarth.* [ab]

Rough, capillary-active surfaces remain demanding substrates for microcontact printing (μCP), as the diffusive mobility of the ink thereon drastically limits the printing resolution. To reduce ink smearing, we developed a polymer-supported μCP, which includes a stamp with a polymer brush-decorated surface. The ink molecules are thereby bound into the stamp-bound brush matrix, from where they may be transferred to the substrate, which exclusively occurs during the contact of both interfaces. Conventionally, Slygard184-based polydimethylsiloxane (PDMS) stamps are used for μCP. The material's surface must be functionalized in a multi-step procedure for the protocol. In addition, Sylgard comes along with a drawback of a persistent leakage oligomeric PDMS (oPDMS), which can contaminate the substrate. To circumvent these problems, we developed a novel stamp material, that (i) enables a straightforward polymer grafting, and (ii) shows a low tendency of oPDMS leakage. We prepare the stamp with a commercially available amino-functional PDMS prepolymer, and a polymer-ic crosslinker that can be used for a controlled photoiniferter reversible addition and fragmentation chain transfer (PI-RAFT) polymerization. The prepared stamp shows elastic properties at the relevant strain region, is compatible with brush formation, and has been demonstrated demonstrated suitable to transfer precise patterns on rough capillary-active oxide surfaces.

1. Introduction

Microcontact printing (μCP) has gained increasing interest in various fields including regenerative medicine,[1,2] microelectronics,[3,4] or biosensing[5,6] among others. Being a prominent technique within the field of soft lithography,[7] μCP has shown great potential due to its ability to pattern surfaces with a variety of materials at the microscale.[8,9] The technique involves an elastomeric stamp, which is used to transfer micropatterns of functional molecules onto different substrates *via* a contact-mediated transfer.[10] Developed in the early 90s by Kumar and Whitesides, μCP was initially used to create microarrays of thiol-based self-assembled monolayers (SAMs) on smooth gold substrates using patterned stamps.[11] Since then, μCP has been used to create microstructures of functional materials such as alkylsilanes,[12] amines,[13,14] and complex macromolecules,[15,16] which have found a variety of different applications. μCP has become an increasingly popular technique for microscale surface patterning due to its experimental feasibility,[17] its potential for cost-effective manufacturing,[10] scalability,[3,18] and the versatility in printing on various surface topographies.[17,19] μCP is advantageous being relatively simple, fast, and inexpensive compared to other microscale surface patterning techniques, such as photolithography,[20] electron-beam lithography,[21] and dip-pen nanoimprint lithography.[22,23] Accordingly, photolithography is tedious and is accompanied by an intrinsic resolution limitation, e-beam and nanoimprint lithography techniques often require expensive instrumentation and are time-consuming. Nowadays, μCP is frequently used for fabricating microelectronic[24] or microfluidic devices[25] or for autonomously studying cell differentiation and proliferation[16,26] that require patterned microstructures. For creating such microstructures, classically, polydimethylsiloxane (PDMS) is used as an elastomeric stamp material.[10] Even though a number of other polymeric materials have also been used to fabricate stamps for different applications, such as agarose,[27] poly(urethane acrylate),[28] etc., PDMS plays a predominant role here. Its widespread use can be explained by the useful properties of PDMS, such as a high elasticity, a good chemical and thermal stability as well as optical transparency.[29] Despite the extensive use of PDMS as an elastomeric stamp material in μCP, the leakage of oligomeric PDMS from the matrix poses a significant challenge. As an example, oligomers were detected in PDMS-based microfluidic systems, which

have been applied during cell culture experiments. These PDMS species have been found in cells, which bears the potential for data misinterpretation in cell studies.[30],[31]

Another study has demonstrated a linear relationship between the loss of oligomeric polydimethylsiloxane (oPDMS) and the swelling ratio when dissolved in various organic solvents.[32] Accordingly, species that are not incorporated into the PDMS network during the curing process diffuse out of the stamp material, also during the printing process, which contaminates the patterned areas to a significant extent.[33–35] As an example, SAMs of hexadecane[34] or dodecane thiols[35] were formed on gold substrates with μCP using a PDMS stamp. X-ray photoelectron spectroscopy (XPS) revealed a significant amount of PDMS on the printed gold substrate, along with thiols. Even though it was suggested that thorough washing of PDMS stamps prior to printing could potentially mitigate the PDMS leakage issue, PDMS transfer could not be entirely prevented.[35]

For μCP, usually, substrates such as Au,[[11,36] Ag,[37],Cu,[38],Pd,[39] etc. are used, which are patterned with SAMs. These substrates are characterized by their smooth surfaces. Rough, or capillary-active substrates, however, are not as straightforward to print on. While ink molecules can be transferred with precision to smooth substrates, particularly if they possess an excellent affinity to the substrates, there can still be lateral ink spreading caused by ink mobility on non-smooth substrates.[18] This renders precise printing on rough surfaces is demanding. Even though an effective transfer of proteins[40] or polymers[41] has been reported to be successful on rough surfaces such as porous silica[41,42] or thin polymer foils,[43] it would be beneficial to obtain an accurate pattering to circumvent ink smearing and poor printing precision, along with a high chemical functionality of the printing area. For this purpose, we described a μCP technique that utilizes polymer-supported ink transfer to achieve a high accuracy on rough, capillary-active surfaces.[44] In particular, Akarsu *et al.* optimized the process for the transfer of functional alkoxysilanes.[45,46]

Accordingly, a hydroxyl group-containing poly{N-[tris(hydroxymethyl)methyl]acrylamide} (PTrisAAm) polymer was grafted from the PDMS stamp using by reversible addition-fragmentation chain transfer (RAFT) polymerization to immobilize 3-aminopropylethoxysilane (APTES) as an ink covalently. Printing was carried out with the functionalized stamp on capillary active oxide surfaces, which showed a precise pattern transfer from the stamps to substrates. A significant benefit from this method is the high functionality of the patch area, which offers primary amino functionalities for further functionalization. However, stamp functionalization using this method is relatively time consuming.

In this study, we aim at overcoming two obstacles: the oligomeric PDMS leakage, as well as complexity and time requirement of stamp production. Both issues are tackled by developing a novel stamp formulation that can be prepared in a straightforward fashion. To create a functional stamp precursor material, polymeric crosslinkers containing xanthate end groups are synthesized and combined with a functional polydimethylsiloxane (PDMS) prepolymer. This stamp material can be advantageous for μCP, exhibiting comparable properties to conventional PDMS, along with a lower tendency to oligomeric PDMS leakage from the matrix. As we have used PI-RAFT polymerization for the preparation of the crosslinkers, these short-chain polymers introduce reactive sulfur species into the polymeric framework.[47,48] We show that these xanthates can be re-activated using PI-RAFT, by exposing the stamps to an aqueous monomer solution and activate the xanthate with light. The resulting polymer matrix forms at the stamp surface, which can be used for a polymer brush-supported μCP process.[45] The strategy enables grafting of the stamp directly after production, rendering tedious functionalization protocols unnecessary.

2. Results and discussion

In this study, we prepare a PDMS-based elastomeric stamp suitable to be utilized for a polymer-brush supported microcontact printing (μCP) routine for the precise patterning of capillary-active oxide surfaces (**Scheme 1**). The μCP routine relies on the transfer of 3-aminopropyl(triethoxy)silane (APTES), used as the ink for μCP, to the substrate, which occurs merely, when the stamp and the substrate are brought in direct contact with each other. For this purpose, the stamp surface is equipped with a polymer offering a trivalent hydroxy binding site, to which the active silane ink can bind in a covalent fashion. Immobilized therein, it may be transferred to the substrate during microcontact as a result of the dynamic nature of this bond, where it

then binds in an irreversible fashion. In this study, we want to fabricate a tailor-made PDMS stamp, which (i) enables a straightforward polymer grafting, and (ii) shows a low tendency of oPDMS leakage.

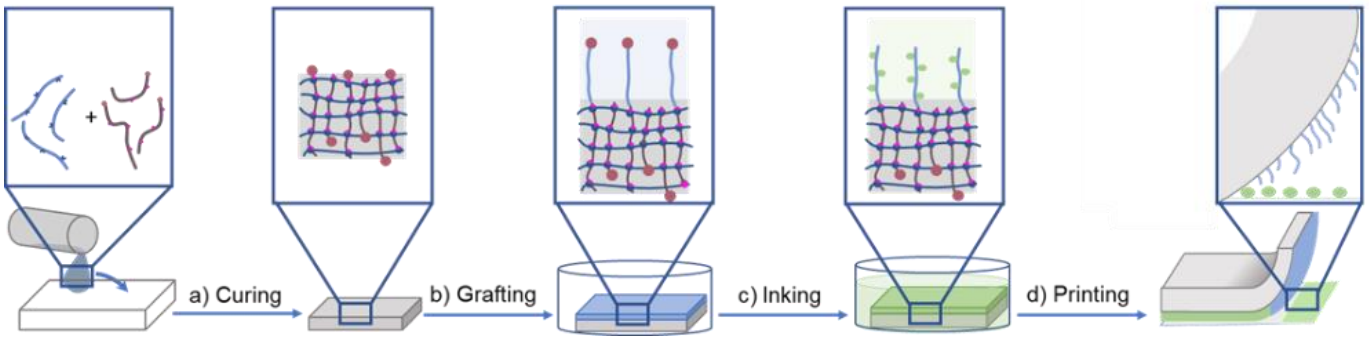

Scheme 1. Schematic illustration of the overall µCP process. a) Polymer precursors are used for casting the stamp. After curing, a cross-linked stamp is obtained. b) In an aqueous solution, a grafting process is induced using PI-RAFT. c) The hydroxy-containing polymer chains react with APTES used as an ink. d) The inked stamp is used for the printing process.

Accordingly, we first aim at preparing a suitable stamp, whose surface can directly be subjected to a grafting procedure to attach the polymer matrix. A polymeric network is formed by combining a PDMS-based prepolymer with a polymeric crosslinker (**Scheme 1a**). The crosslinker is thereby synthesized via PI-RAFT polymerization using a xanthate as iniferter.[49] With polymers featuring xanthate end groups incorporated into the PDMS, the matrix contains functional groups that can be re-activated by light to extend the polymer chains of the crosslinker upon the addition of a new monomer. Polymer brushes are grafted explicitly from the active surface of the stamp when the polymerization is conducted in an aqueous environment. Here, the surface-selectivity is ensured by the fact that the water-soluble monomers cannot diffuse into the hydrophobic stamp material (**Scheme 1b**), which, in turn, prevents the polymerization inside the stamp body. With that method brushes of {N-[tris(hydroxymethyl)methyl]acrylamide} (TrisAAm) can be grafted from the surface. Due to the hydroxy binding sites in their side chains, APTES can be coordinated side-on thereto, which is used as the ink for µCP (**Scheme 1c**).[45] With the incorporated amino group, any available functionalities can be bound covalently to the ink. During the process of µCP, said functionalities are transferred to the substrate (**Scheme 1d**). The subsequent paragraphs provide a comprehensive description of the formation and properties of the stamp, surface modification through grafting, and printing using the stamp.

Stamp Preparation

To prepare the novel stamp and circumvent the oPDMS leakage problem, we use a PDMS precursor material compatible using a custom-made crosslinking chemistry. By using multiple reactive units per prepolymer and cross linker, in combination with a highly efficient coupling chemistry, we aim for a quantitative incorporation of macromolecules into the network. For this purpose, we use a commercially available 6-7% aminopropylmethylsiloxane-*co*-dimethylsiloxane (poly(6-7%APMS-*co*-DMS) precursor that has amine functionalities in its side chain. These amino-functions can be utilized for crosslinking, using a crosslinker with *N*-hydroxysuccinimide (NHS) ester side chains to form amides. The polymer precursors can be cast using a mold into a preferable shape, where they can be cured to fabricate a microcontact printing stamp.

For this purpose, first, a crosslinker polymer was synthesized using PI-RAFT polymerization. The crosslinker is a copolymer composed of butyl acrylate (BA) and *N*-acryloxysuccinimide (NAS, synthesis of NAS confirmed by ^{1}H-NMR, **Figure S1**), in a 4:1 ratio. Comprising of 20% NAS in the polymer chain, the polymer facilitates crosslinking, whereas butyl acrylate would not interfere with said process, while imparting desirable flexibility to the final material.[50] Poly(80%BA-*co*-20%NAS) was synthesized using a xanthate as a chain transfer agent (CTA) in bulk (**Figure 1a**). The PI-RAFT polymerization was selected due to its simplicity, efficacy in producing polymers, and its adaptability in accommodating a diverse range of monomers.[47,49] We targeted a low degree of polymerization (DP) during the preparation. Accordingly, polymers with a varied

range of DP 10, 20, 30, and 50 were synthesized (polymers **P1-4** respectively, **Table S1**). A conversion of above 98% was recorded from NMR analyses. The molecular weight (M_n) and dispersity (Đ) were determined by SEC. M_n, for a polymer with a targeted DP of 20 (**P2**) was recorded at 2600 g mol^{-1} and its Đ was found at 2.05 shown in **Figure 1b**. The corresponding characterization data (M_n & Đ) of all the synthesized crosslinkers (^{1}H NMR, size exclusion chromatograms, SEC) are displayed **in Figure S2** and **Table S1**. A broad molecular weight distribution was expected as the chain transfer coefficient of the used xanthate with BA is very low.[46] Nevertheless, the xanthate end groups are expected to be incorporated into the network.

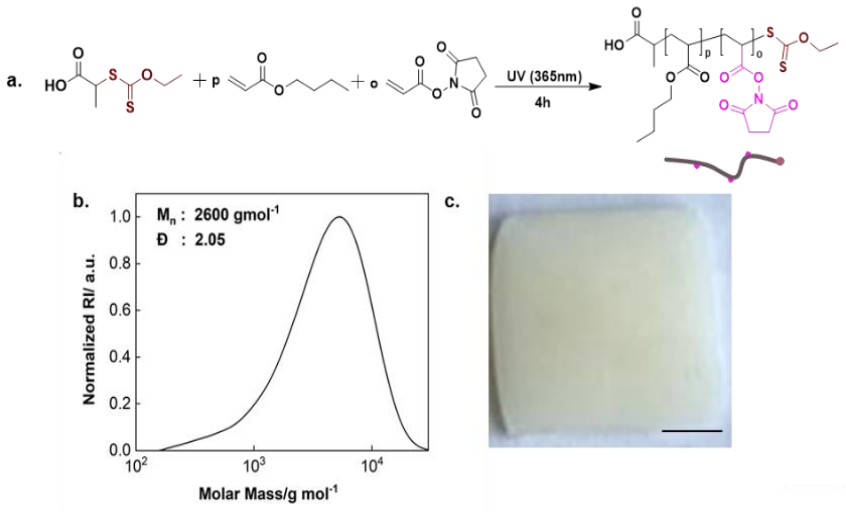

Figure 1. Preparation of poly(butyl acrylate-co-N-acryloxysuccinimide) used as a cross-linker of the PDMS chains. a) Reaction scheme. b) SEC profile of poly(80%BA-*co*-20%NAS) for a targeted DP 20 (SEC was performed in THF, polystyrene (PS)-standards). c) A photograph of the novel stamp. The scale bar is 2.5 mm.

After successful synthesis of the crosslinkers we employed them (longer to shorter chain; in this order) for stamp preparation. For this purpose, the crosslinking polymers are blended with the precursor PDMS. The low DP polymers **P1** and **P2** (DPs of 10 and 20) performed best in terms of handling of the materials, as these polymers are viscous liquids, we can be poured and mixed in a straightforward fashion. In contrast, the longest copolymer (**P4)** showed waxy characteristics, which made it difficult to add to and mix with the precursor PDMS. Copolymer **P3** followed a similar trend but performed better than the former. Dissolving the polymer in either a volatile or a non-volatile solvent eased up the process, however a crooked stamp or a sticky stamp was obtained on most occasions, which we attribute to a too quick evaporation of a volatile solvent or incomplete removal of residual high boiling-point solvent within the mixture, respectively **(Figure S3**). Note, that any contamination of a solvent gave poor curing results of the stamp, which motivated us to omit any solvent during the polymerization of poly(80%BA-*co*-20%NAS) or during the mixing of the precursor polymers.

For the following investigations, **P1-P3** were used to create networks (**Table S2).** The addition of the crosslinking polymers to the PDMS prepolymer rapidly provided a crosslinked PDMS material. The rapid crosslinking process, however, represents a pivotal drawback during the casting, as the precursor material does not have enough time to cast the mould before it solidifies. To avoid this, the reactive primary amines of the PDMS prepolymer were protected by protonation with formic acid. As cationic ammonium salts, the PDMS side chains do not react with the NAS moieties, enabling the handling of the liquid precursors. The formed cationic ammonium salt decomposes residue-free into water and carbon monoxide at elevated temperatures. A simple treatment of the stamp at a higher temperature would remove the protection group (**Figure 2**), and, therefore, enable the crosslinking process.

Accordingly, the crosslinker was added to the protonated prepolymer and treated at a temperature of 90 °C for curing (**Table S2**). To assess an optimized molar ratio of NHS-active ester to amino functionality (in its protonated form), we varied it from 0.25 to 1.6 At a ratio below 0.5 or above 1, incomplete crosslinking was observed, which became obvious as the sample remained sticky (**Figure S3**). When the ratio was kept between these values, the cured stamp was opaque in nature and flexible enough for microcontact printing.

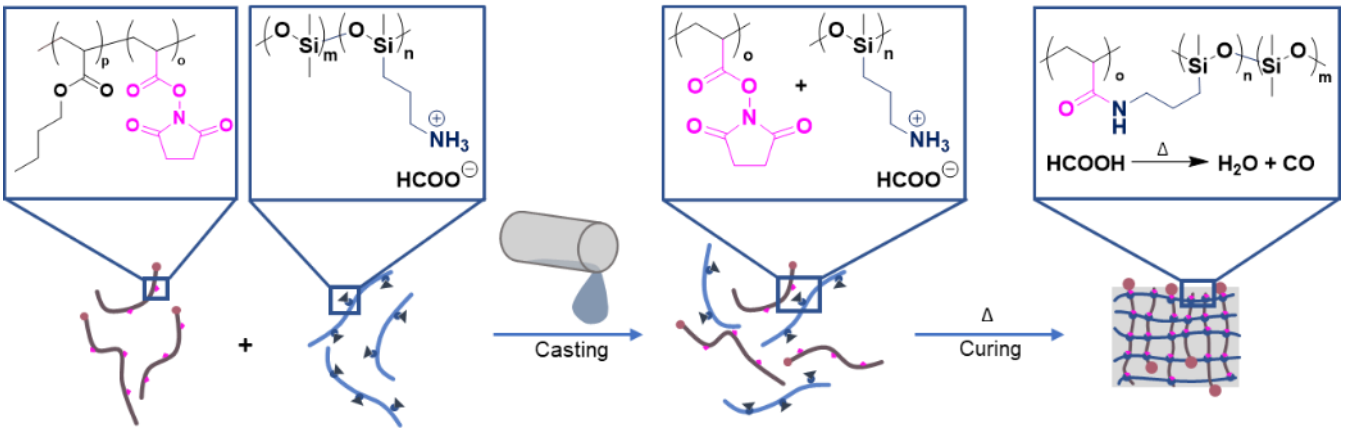

Figure 2. Illustration of novel stamp preparation process. Protonated 6-7%APMS-*co*-DMS crosslinks with NAS when mixed and cured.

Swelling Properties & oPDMS Leakage of the Stamp

To obtain a comprehensive insight into the crosslinking properties of the stamp, we conducted a set of different experiments with various stamps (**St1** – **St14**; divided in 14 categories based on different NAS-to-APMS ratio**,** see **Table S2**). A first indication for the crosslinking efficiency was determined already qualitatively by evaluating the stickiness of the material during stamp preparation. Since the first inspection of the stamps revealed that cross-linking was optimal between the range of 0.5 to 1 (NAS-to-APMS), to obtain a more quantitative insight into the results for the optimized ratio, swelling experiments were conducted with representative stamps. Accordingly, different samples were swollen in toluene, which represents a common solvent for both PDMS and acrylate-based prepolymers. After a quick removal of the excessive toluene, thereby placing the stamp in a small plastic tube and removing the supernatant liquid by centrifugation, the relative swelling degree is determined as the mass increase of the stamp after soaking. Subsequent drying of the stamp at elevated temperature and reduced pressure provides access to the gel fraction of the crosslinked material, which is indicative for non-crosslinked polymer that was removed during the toluene washing. To correlate the swelling properties of the stamp with the characteristics of the crosslinking polymers **P1**-**3**, we kept the NAS-to-APMS ratio constant at 0.5 during all experiments. Swelling tests carried out with a stamp prepared with **P3** (longest chain), demonstrated lower weight loss than the stamp containing a crosslinker of **P1** (shortest chain) (**Figure S4**), pointing toward a more efficient crosslinking of the material, when longer crosslinking chains are used. The greater weight loss observed for low M_n stamps might be explained by the presence of fewer crosslinking sites in their chains. Nevertheless, the crosslinker with a DP of 10 had superiority in terms of handling during stamp preparation. Considering both ease of handling and weight loss characteristics, stamps prepared with the crosslinker **P2** (DP of 20, **St4** & **St5**, see **Table S2**) were prioritized for all further experiments, which provided the optimal trade-off between the fluidity of the crosslinker polymer and optimal gel properties of the stamp. Next, the effect of the curing temperature was evaluated. For this purpose, initial swelling tests were carried out with sample **St4** (containing **P2**) which were cured at 90 °C **(Figure 3a).** The stamp showed a gel fraction of 91 ± 3%, and a swelling degree of 65 ± 4%. Subsequently, a similar swelling test with another sample, **St5** (cured at 110 °C) was performed. Note, that no prior washing step was carried out before the swelling tests. Here, similar characterization values were observed. For comparison, a conventional Sylgard PDMS was prepared (refers to **CSt1**), which uses a prepolymer-to-crosslinker ratio of 10:1 and has been cured at 110 °C. Possessing a similar swelling behavior as well as a comparable gel fraction right after the preparation (**Figure 3a**), both samples differ in their long-term behavior. Accordingly, a major drawback of a PDMS stamp is represented by the fact, that Sylgard-based polydimethylsiloxane (PDMS) stamps exhibit a persistent release of oligomeric PDMS. This weight loss is a prevalent occurrence in such stamps and can result in the contamination of the printing substrate.[34,35] For

quantification of the PDMS release, a long-term experiment was designed to compare the weight loss profiles of the novel and the conventional PDMS-based stamps. In detail, we performed swelling experiments on the previously dried stamp samples **St4**&**5** and **CSt1** that already underwent the first wash (week 1). The experiments were conducted at weekly intervals for a period of another three weeks to monitor any variations in weight among the samples over time (**Figure 3b**). Although, the weight loss patterns of the samples indicated that both **St4** and **St5** experienced a higher initial weight loss (%) directly after production, in comparison to **CSt1**, a negligible weight loss (%) was observed for the novel stamps in the second week, resulting in no further weight loss after the third and fourth weeks. In contrast, despite exhibiting a low initial weight loss (%) after the first wash, **CSt1** demonstrated a consistent trend of weight loss in the second, third, and fourth weeks. As a result, the novel stamp has a greater potential to mitigate the risk of contaminating the printing surface through the release of contaminants from the stamp, in contrast to conventional stamps.

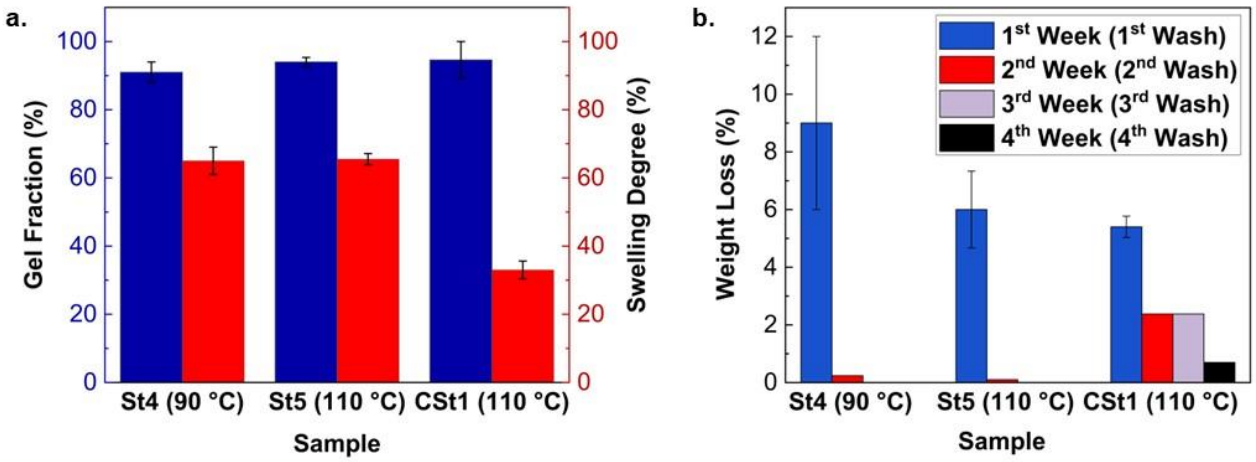

Figure 3. a) Gel fraction and weight loss (%) of novel (**St4**&**5**, cured at 90 °C & 110 °C respectively) and PDMS (**CSt1**, cured at 110 °C) stamps. Gel fractions are 91 ± 3%, 94 ± 1.33%, and 94.6 ± 0.37% respectively (**St4**, **St5**, & **CSt1**). b) Weight loss profiles of **St4**&**5** and **CSt1** over 4 weeks. The first wash was considered as the weight loss (%) of the first week directly after production. Weight loss (%) of first wash are recorded at 9 ± 3%, 6 ± 1.33%, and 5.4 ± 0.37% respectively for **St4**, **St5**, and **CSt1**. Same samples were used for further washing in week 2-4 in toluene (one representative sample was selected from each group).

Mechanical Properties

For characterization of the viscoelastic properties of the materials, we performed dynamic mechanical analyses (DMA) of the cured stamp. For this purpose, we used an oscillatory strain at a frequency of 10 Hz. The behavior of the stamp under compressive force can provide an improved understanding of the printing process, during which the stamp is exposed to a compressive force as well. Since a printing force of no more than 2N (Newton) is applied to a stamp area of ~ 100 mm^2, the stamp is supposed to withstand a theoretical stress of around 0.02 MPa. Accordingly, we subjected our stamp (**St5**) to a dynamic force of F_{dyn} ~ 2N with a temperature ramp up to 150 °C for a duration of 25 min. **Figure 4a** reveals, that the novel stamp demonstrates an elastic behavior with a storage modulus (E') of 1.2 MPa at room temperature, which declines as the temperature increases until it reaches a plateau at 0.63 MPa at 146 °C. It indicates that the material possesses adequate elasticity and a low viscous component, as outlined by a low loss modulus (E'') as well as a low phase mismatch as characterized by tan δ (for comparison, the viscoelastic behavior of PDMS is shown in **Figure S5a**). In conclusion, the viscoelastic characteristics point toward a mainly elastomeric material at a range relevant for µCP, which renders the material a sufficient elastomer for our method. To obtain a further insight into the stamp mechanics, the viscoelastic behavior was also determined in tension mode. There, **St5** is exposed to an axial oscillatory force with a frequency of 10 Hz as well. The data reveals a storage modulus E' of 0.7 MPa at room temperature (**Figure 4b**), however, a rise with increasing temperature indicates enhanced crosslinking after temperature > 130 °C. In analogy to the data obtained in compression mode, also a negligible viscous component E'' (along with a low phase mismatch) is observed. A corresponding tension profile of PDMS (**CSt1**) is also shown in **Figure S5b**. We further investigated the tensile properties of **St5** and PDMS (**CSt1**) by measuring uniaxial tensile behavior in a quasi-static manner (**Figure S6**). Our stamp material shows

flexibility, with a Young's modulus of 0.68 ± 0.4 MPa and the highest tensile strength for novel stamp is observed at 0.14 ± 0.01 MPa respectively (for comparison, the tensile characterization of PDMS is outlined in **Figure S6** as well). However, an elongation at break of 24.1 ± 0.4% is recorded. The elastic properties of the stamp, experiencing a small stress during printing, are therefore well compatible with the printing.

These data, altogether, reveal an elastic behavior of the produced stamp in both compression and tension mode, which renders it well-compatible with our µCP application.

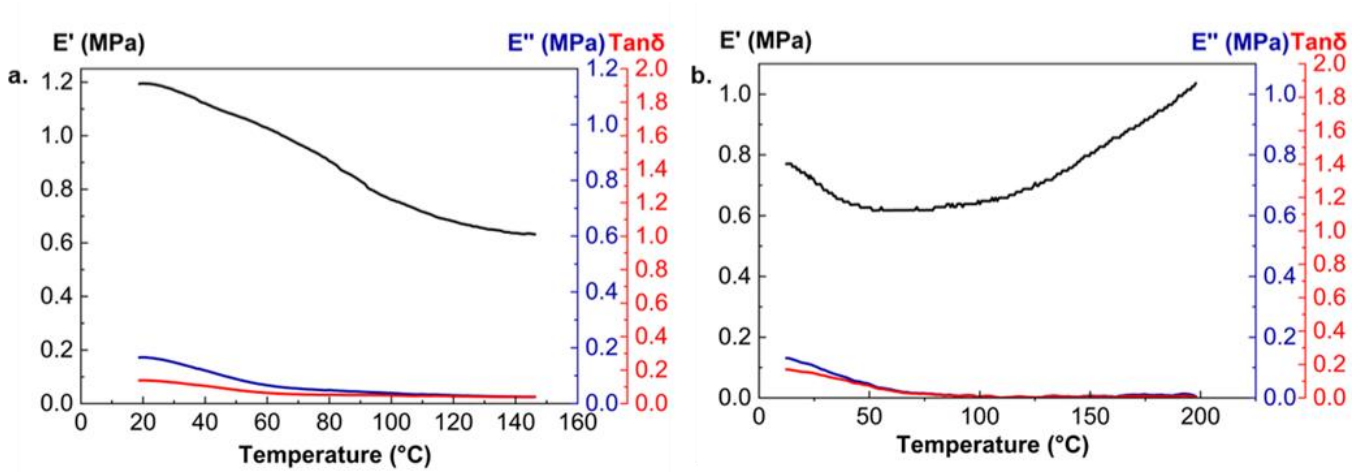

Figure 4. Dynamic mechanical analyses of novel stamp material. a) Compression profile. A dynamic force (F_{dyn}) was applied on a sample size of ~ 0.9 cm^2. b) Tension Profile (10 Hz, 5 K min^{-1}).

Surface Modification

In order to apply the µCP protocol as described by Akarsu *et al.*,[45] we need to install PTrisAAm brushes at the stamp surface. As the crosslinker polymers **P1**-**4** are prepared by PI-RAFT using xanthate CTAs, the stamps inherit functional CTA moieties at their surfaces, which are directly used for surface grafting (**Figure 5a**). For grafting, we expose the stamps to an aqueous monomer solution, which includes a small amount of the dissolved xanthate CTA as well. Upon irradiating the solution with UV light (365 nm), a polymerization of TrisAAm is induced. The additional CTA in solution acts, in this context, as a shuttle CTA. Owing to the hydrophobic nature of the stamp, which impedes the penetration of water into the PDMS framework, it can be expected that polymerization occurs exclusively at the stamp surface. To probe the characteristics of the formed polymer brushes, polymers formed simultaneously in solution were characterized *via* SEC. Since the CTA-shuttled PI-RAFT polymerization was used, the polymer formed in solution is expected to possess similar properties to the polymer brushes attached to the surface due to the controlled transfer of radicals to different areas of the surface during the reaction.[51] The corresponding SEC trace can be found in **Figure S7** and **Table S3**.

For further characterization of the stamp surface, contact angle measurements were conducted. The contact angle measured before grafting averaged to a value of 121 ± 6° due to the hydrophobic nature of the stamp material (**St4**, cured at 90 °C). After PTrisAAm brushes were grafted from the surface, the contact angle significantly decreased to 40 ± 9° (**Figure 5b&C**). As aforementioned, polymer in the solution was characterized via SEC. The number-average molecular weight (M_n) was determined to be approximately 187 kg mol^{-1}, with a targeted degree of polymerization (DP) of 1500. The dispersity (Đ) was found to be around 6 (**Figure 5d**). Note, that a high dispersity in polymer brushes can be an advantage, as this increases the contact area of the interface.[52]

When using the stamp cured at 110 °C (**St5**) the grafting efficiency was lower, as expressed by a contact angle of 80 ± 22° (**Figure 5C**). We explain this result with the inactivation of the xanthate group at this temperature, leading to a less efficient brush formation. At a lower temperature and shorter curing time, the xanthate

remains stable producing better results in terms of polymer grafting density from the surface, as it is characterized by a decreased contact angle. Despite performing lower regarding the cross-linking efficiency (as it is characterized by the gel properties), we choose a curing temperature of 90 °C, as it was the best trade-off between the gel characteristics of the stamp and the efficiency to graft polymer brushes from its surface.

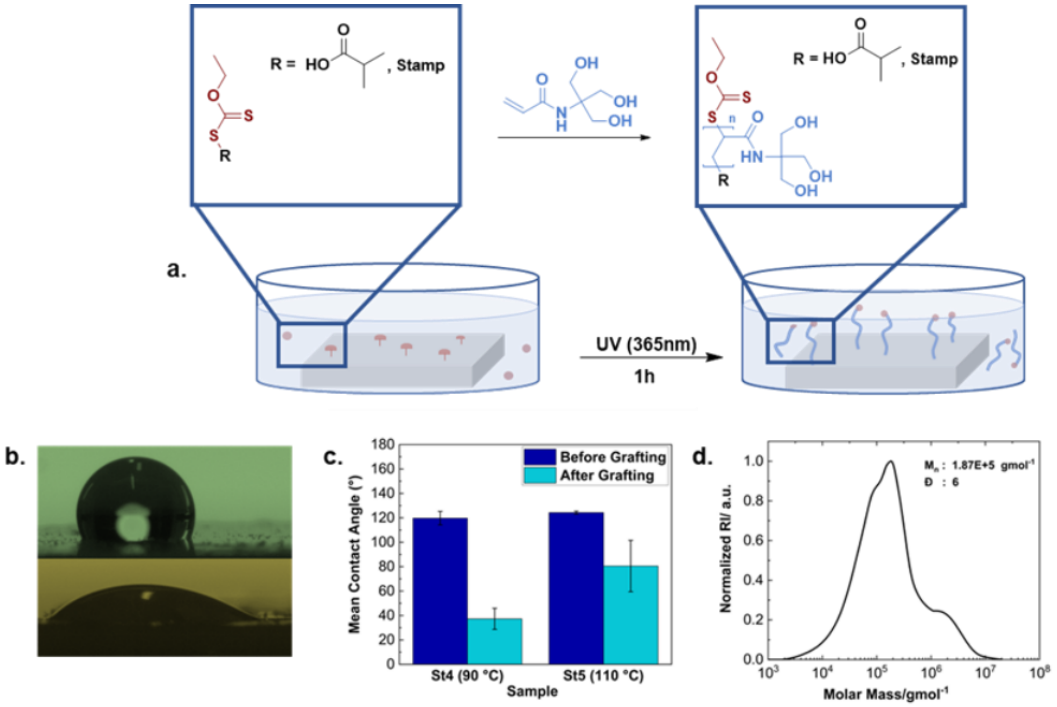

Figure 5. a) PTrisAAm grafting scheme (CTA in maroon, grafted PTrisAAm in blue). b) Contact angle measurement before (top) and after (bottom) grafting with PTri-sAAM (2 µL Water drop, **St4**). c) Mean contact angle before and after grafting PTrisAAm from novel stamps (**St4**; cured at 90 °C and **St5**; cured at 110 °C). d) SEC profile of PTrisAAm in the solution representing the nature of the polymer formed on the stamp's surface due to shuttle CTA approach. An aqueous solution with 0.3 vol% formic acid, and 0.1M NaCl was used as SEC eluent (PVP-calibration).

Inking and Printing

Alkoxy silanes are effective as functionalization agents on oxide surfaces, where they can be subjected to further functionalization,[53] which qualifies them to be a suitable ink for our printing method. Due to the trivalent nature of silicon in the structure of APTES, they can be tethered to a polymer offering hydroxy binding sites in their side chains, such as said PTrisAAm polymer brushes, where they bind in a reversible fashion. Forming stable bonds to hydroxy-terminated oxide surfaces, they can be used to introduce amino-functionalities to said substrates, which can be used for the further functionalization with organic or inorganic molecules (**Figure 6a**).[54] A similar procedure as we described in our previous study[45] was replicated for the novel stamps to attach APTES to the surface-grafted polymer brushes. After successful ink attachment, microcontact printing was carried out on a smooth surface for analysis. To characterize the surface chemistry, an activated surface oxidized Si wafer was selected as the ideal substrate for printing (corresponding Si 2p spectra is shown in **Figure S8a)**, and a smooth inked flat stamp (**St4**) was applied thereon. The transfer of APTES as ink was evaluated by XPS. The characteristic asymmetric peak for N (1s) corresponding to its binding energy at ~ 400 – 405 eV was observed (**Figure 6b**; note, that the signals are corrected as they appear downfield shifted, which is a result of an overcompensation from the charge neutralizer of the XPS device). Within this region, signals characteristic for non-protonated ($-NH_2$) and charged amino groups ($-NH_3^+$) are found. These results clearly indicate that the amino functions have been transferred from the stamp to the substrate. In addition, elemental analysis of the XPS data of a plasma-treated Si wafer and APTES-printed Si wafer were compared. The latter shows trace of nitrogen content which clearly indicates the APTES transfer to Si wafer substrate (**Figure 6c**), along with significantly enhanced amounts of carbon, also indicating the transfer of APTES. C (1s) signals seen prominently from ~ 284 to ~ 290 eV (**Figure S8b**) were also investigated which shows characteristic C-C and C-N regions to confirm APTES transfer. Moreover, the curve also resembles with the model curves (shown in **Figure S8c, & d**), representing characteristic peaks for APTES.

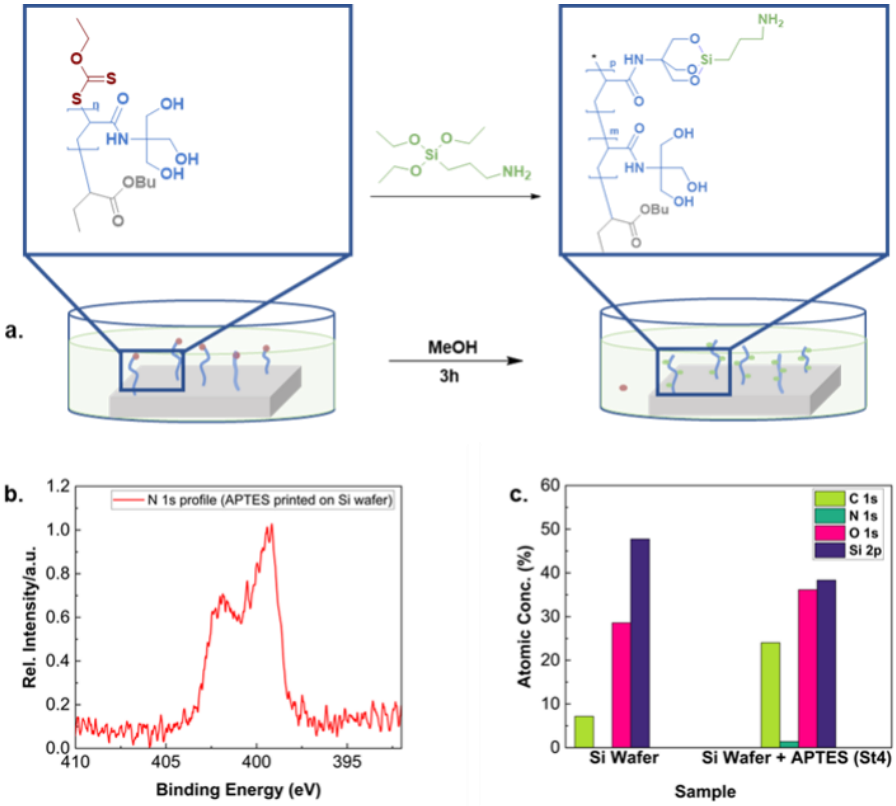

Figure 6. a) Scheme representing APTES ink (in green) attachment to grafted PTrisAAM polymer (blue) from novel stamp (**St4**). '*' denotes that the xanthate group is likely to be cleaved off the polymer in the solution. b) N (1s) spectra demonstrating APTES transfer to Si wafer. c) atomic concentration (%) of elements presents on the plasma-treated (left) and APTES-printed Si wafer with **St4** (right).

To demonstrate the precision and accuracy of the µCP process on a rough capillary-active surface, we prepared patterned stamps (4 µm stripe pattern, patterned stamp is shown in **Figure S9a**) to print on a silica-gel modified glass substrate with a roughness, Sq of ~ 93 nm (AFM height image is depicted in **Figure S10a**). Accuracy of ink transfer was evaluated by a comparative printing experiment performed with a bare stamp, to which non-covalently bound Rhodamine 6G (R6G) was added as an ink by drop-casting. In comparison, we used a PTrisAAm-grafted stamp inked covalently with APTES and labelled it with fluorescently active Rhodamine B isothiocyanate (RBITC). Here, the positively charged Rhodamine dyes are particularly prone to ink smearing due to electrostatic attractions to the negatively charged silica gel substrates. The printed substrates were analysed with fluorescence microscopy to probe the printing pattern. Evidently shown in **Figure 7a & b**, ink (APTES) transfer to the silica-gel modified glass substrate from the grafted stamp surface is more precise (**Figure 7b**). In Figure 7b, thinner stripes are observed than in Figure 7a, where the transfer of non-covalently attached R6G ink due to less or no ink smearing. Note, that the consistency of the stripe pattern can be explained by the soft characteristics of the stamp, which allows a more efficiently adaption to the rough surface topology of the substrate to compensate uneven surface characteristics. To further show the versatility of the printing process we used a tailor-made mould, which we created with stereolithographic 3D printing. As outlined in **Figure 8a**, the mould possesses structural details in the low µm range as also shown in the light transmission micrographs (**Figure 8a, i, & ii**). The cast stamp possesses a similar wealth of structural details, which are well-preserved after the stamp replication (**Figure 8b**, **iii**, & **Figure S9b** & **c**). The stamp, after inking, is subjected to µCP. For visualization of the printing pattern, we exposed the printed area to an NHS-ester based Alexa 555 dye, which represents a potent probe for fluorescence microscopy. Noticeable patterns were observed under a fluorescence microscope (**Figure S9d**), using a plasma-activated smooth Si wafer as a substrate.

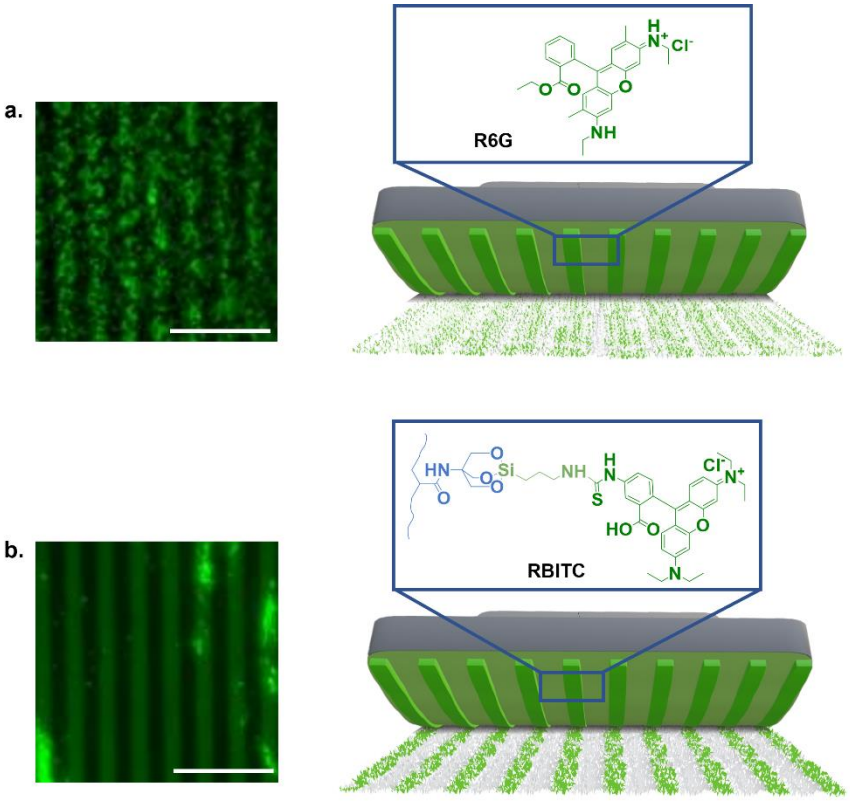

Figure 7. Printing with patterned stamps. a) Fluorescence microscopy image of printed stripe patterns on silica-gel modified glass with bare stamp inked with R6G (non-covalently attached ink). b) Printed stripe patterns on silica-gel modified glass with grafted stamp inked with covalently attached APTES (Labelled with RBITC). Scale bars are 20 µm.

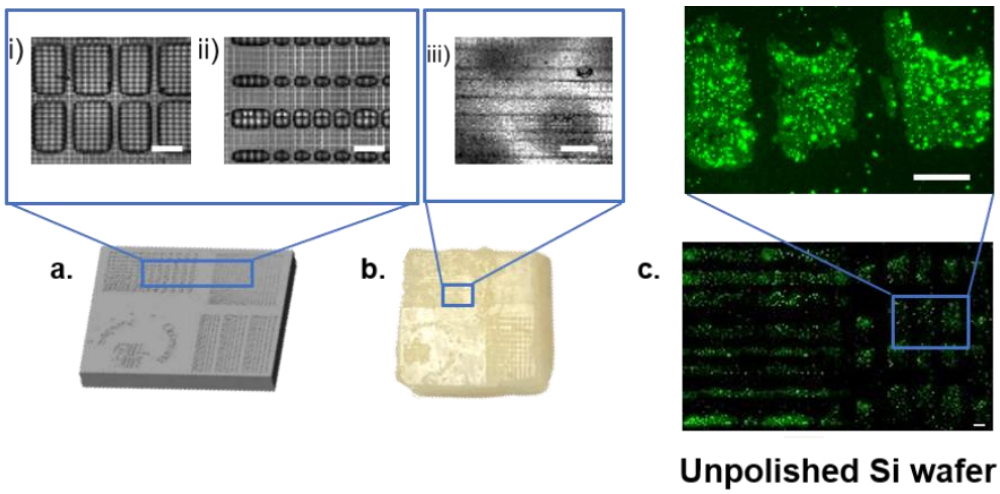

Figure 8. a) CAD Design of 3D printed mold with different structural patterns. The zoomed in area shows light microscopy images of the patterns (i & ii). b) Photography of a patterned stamp. Zoomed in area 'iii' shows light transmission image of patterned stamp surface. c) Fluorescence micrographs of printed patterns on a rough Si wafer. Zoomed in area on the top row indicates that the substrate was post-labelled with Alexa555 fluorescence dye. Images of patterned surface are also shown in **Figure S9a, b & c**. Images are stitched, gamma value (0.38) and brightness corrected on ImageJ. Scale bars are 20 µm.

To demonstrate further the suitability of our method of printing patterns on various rough surfaces, we used an unpolished side of a Si wafer as a substrate, which possesses a roughness of $S_q \sim 105$ nm (AFM height image is shown in **Figure S10c**). The surface of the smooth Si side of the wafer was confirmed with AFM as well (root mean square roughness, $S_q \sim 0.48$ nm, AFM height image shown in **Figure S10b**). **Figure 7e** reveals a well-structured pattern transfer from the stamp to rough wafer surface. Here, also a larger area of printed details is observable. These patterns remain stable, even after thorough washing. This feature indicates the covalent binding of the APTES to the surface.

3. Conclusions

In summary, we developed a novel microcontact printing stamp based on amide crosslinking chemistry. A commercially available reactive amino-containing 6-7%APMS-*co*-DMS was combined with a xanthate end groups-containing polymeric crosslinker, poly(80%butyl acrylate-*co*-20%*N*-acryloxysuccinimide), to obtain an elastomeric stamp material *via* amide cross-coupling. Afterwards, the swelling and the mechanical properties of the stamp were determined. We found that this novel stamp shows a much lower tendency to oligomeric PDMS leakage when compared to conventional stamps, thus, overcoming the limitation of conventional stamps that contaminate the substrate area during the µCP process. Our crosslinker was synthesized using photoiniferter RAFT polymerization, which allowed for exclusive access to the xanthate end groups on the surface with an aqueous monomer solution and activation with light. We suspended the stamp in a hydrophilic PTrisAAm monomer solution and illuminated it with UV-light for a straightforward grafting process from the surface. This grafted polymer brush was utilized to attach reactive ink such as 3-aminopropyltriethoxysilane (APTES). Therefore, we successfully introduced defined microscale patterns on surface substrates exhibiting high capillary activity and receptive to a silane-based chemistry. Due to the direct availability to xanthate on the stamp surface, polymer grafting is easily achieved and the low oPDMS leakage renders extensive washing unnecessary, thus streamlining the overall procedure drastically. In conclusion, our polymer-supported µCP method is a promising approach for precise patterning of rough capillary-active surfaces while reducing contamination and maintaining printed pattern fidelity.

4. Experimental Details

Instrumentation

NMR Spectroscopy. ^{1}H (400 MHz) spectra were recorded on a Bruker spectrometer in DMSO, d_6. The spectra were calibrated on the residual solvent peak (2.50 ppm for DMSO (d_6) for ^{1}H NMR). MestReNova (12.0) was used for data evaluation.

Gel Chromatography (GPC). GPC measurements were performed with devices obtained from Agilent Technologies (PSS, Mainz, Germany). For hydrophobic polymer samples measurements were performed in THF and the device was equipped with polystyrene (PS), standard calibration at 40 °C with a 300 × 8 mm^2 stationary PSS SDV linear M column. Measurements in an aqueous solution containing 0.3 vol% formic acid and 0.1M NaCl with a flow rate of 1 mL min^{-1} were performed in polyvinylpyrrolidone (PVP) standards at 40 °C where the device was equipped with PSS NOVEMA Max column.

Dynamic mechanical analysis (DMA). The measurements were conducted with a NETZSCH DMA 242 E Artemis with a heating rate of 5 K min^{-1} in a temperature range between 20 °C and 200 °C, at a frequency of 10 Hz in tension mode. In compression test, a dynamic force of ~ 2 N was applied (with a preload force of 0.1 N) for a temperature range of 20 °C to 150 °C with a temperature ramp of 5 K min^{-1} at a frequency of 10 Hz. A rectangular sample with dimensions of about 20 × 2 × 2 mm (l × w × t) was selected for DMA measurement in tension mode. A sample size of ~ 0.9 cm^2 was used for compression test.

Tensile Test. Quasi-static tensile test was performed with a universal tensile testing instrument Zwick Z010 from Zwick GmbH & Co. Samples with dimensions of around 6 × 2 × 2 mm (l × w × t) were prepared and the test was performed at room temperature. A preload force of 0.1 N and a pulling rate of 15 mm min^{-1} were used. The values are reported as an average of three independent measurements. All errors are reported as standard deviation.

Contact Angle measurements (CA). The contact angle measurements were performed with an instrument from dataphysics. For each sample, contact angles were recorded at 5 different spots with the integrated software SCA20 (version 5.0.41).

X-ray Photoelectron Spectroscopy. XPS measurements were performed on AXIS Supra+ (Kratos Analytical, U.K.). The instrument used a monochromatic Al Kα- radiation (300 W) for excitation with an operation take-off angle of 90° and an analysis depth of ~ 10 nm. The data were analyzed using CASA-XPS software.

Light & Fluorescence Microscopy. Microscopy analyses were performed on the instrument from Leica Microsystems. A dry objective of HCX PL FLUOTAR 20x/0.50 and 40x/0.80 were used. Images were analyzed on ImageJ (https://imagej.org) v1.54 f for gamma and brightness correction.

3D printing. Anycubic photon D2 (DLP) 3D printer was used to create a 1 cm^2 mold by stereolithography. The design of the mold was created using Asiga software.

Atomic Force Microscopy (AFM). AFM analysis was carried out by a scanning probe microscope from AIST-NT technology. AFM probe was bought from BudgetSensors (Top150AI-G) to measure pristine Si wafer and silica-gel coated glass substrates. A frequency rate of 0.5 Hz and AC-mode (tapping) were used for the measurements. Images were processed on Gwyddion (v2.61). Levelling data by mean plane subtraction, and rows alignment (polynomial degree kept at zero) were done on each image. Roughness was calculated from the statistical parameters of Gwyddion.

Materials and Methods

Materials. 6-7%Aminopropylmethylsiloxane-*co*-dimethylsiloxane (AMS-163), was obtained from Gelest. The commercially available standard kit of SYLGARD 184 from Dow Corning was used for the PDMS preparation. Tridecafluoro-1,1,2,2-tetrahydrooctyl-1-trichlorosilane, 3-aminopropyl(triethoxy)silane (APTES, > 99.8%), {N-[tris(hydroxymethyl)methyl]acrylamide} (TrisAAm) (contains ≤ 7%, KCl, 93%), butyl acrylate, formic acid, potassium ethyl xanthogenate, 2-bromopropanoic acid (≥ 99%), *N*-hydroxysuccinimide (NHS), triethylamine were purchased from Sigma Aldrich. The inhibitor from TrisAAm was removed by passing through activated alumina from Merck (neutral, Brockmann I). Toluene was purchased from Carl Roth. All other solvents were acquired from Sigma Aldrich. Plasma treatment was carried out using PlasmaFlecto10. A UVL-23R compact UV lamp with a power of 4-Watt (0.12 Amps) from Analytik Jena US was used for photoiniferter RAFT (PI-RAFT) polymerization. Microcontact printer "ZUMO-MCP'' obtained from ZUMOLab GmbH (Wesseling, Germany) was used for printing.

Synthesis of N-acryloxysuccinimide (NAS). N-Hydroxysuccinimide (12.0 g, 86.9 mmol) and triethylamine (14.5 ml, 86.9 mmol) were dissolved in dichloromethane (DCM) (150 ml) at 0 °C. The solution was stirred vigorously and acryloyl chloride (7.76, 95.6 mmol) was added dropwise over 30 min. The mixture was then stirred at room temperature overnight. The solution was filtered and washed with water (2x), $NaHCO_3$ saturated solution (2x) and again with water (2x). The solution in DCM was collected and dried over $MgSO_4$, filtered and the solvent was evaporated under vacuum to give a yellowish powder. The solid is purified via a short frit column (eluent: hexane/ethyl acetate, 1/1, v/v) to obtain pure NAS (8.5g, 57% yield).

Crosslinker synthesis (poly(80%butyl acrylate-co-20%N-acryloxysuccinimide). S-(2-propanoic acid) O-ethyl xanthate (Xan, CTA) was synthesized as reported previously.[49] To obtain a degree of polymerization of 20, 292 mg (1.5 mmol, 1 eq) Xan and 1.02 g (6 mmol, 4 eq) NAS were weighed and taken in a Schlenk flask. 3.43 ml (24 mmol, 16 eq) butyl acrylate (BA) was added into the flask. For 1.02 g (6 mmol) of NAS and 3.43 ml (24 mmol) of BA, crosslinker with DP 10, 30, and 50 were obtained with varying amount of Xan, namely, 584 mg (3 mmol), 194 mg (1 mmol), and 116.4 mg (0.6 mmol) respectively. After dissolving NAS and Xan in BA, the solution mixture was degassed with nitrogen flow for 15 min. The monomer solution was then illuminated with UV light (365 nm, 4W) for 4h.

Stamp formation. 6-7%Aminopropylmethylsiloxane-*co*-dimethylsiloxane (6-7%APMS-*co*-DMS) was mixed with poly(80%BA-*co*-20%NAS). The stamps were prepared with a varying molar ratio of NAS-to-aminopropylmethylsiloxane (NAS-to-APMS). To prepare each stamp for a ratio of 0.5, every 100 mg of 6-7%APMS-*co*-DMS prepolymer (0.093 mmol APMS) was combined with 3.8 mg of formic acid (0.083 mmol, 0.9 eq. to APMS) and mixed. 38.25 mg (contains 0.5 eq. of NAS-to-APMS) of poly(80%BA-*co*-20%NAS) was

thoroughly mixed and the mixture was degassed under vacuum and poured in between two flat glass slides. Each time to prepare stamps with different ratios of NHS-acrylate-to-amino (NAS-to-APMS), a varying amount of poly(80%BA-*co*-20%NAS) was added keeping the formic acid's amount between 0.9 eq. to 1 eq. to APMS. To produce stamps with 0.25, 0.3, 0.75, 0.8, 1, 1.4, and 1.6 of NAS-to-APMS ratio, 19.1 mg, 23 mg, 57 mg, 61 mg, 76.5 mg, 107 mg, and 122 mg of poly(80%BA-*co*-20%NAS) are added to each 100 mg of 6-7%APMS-*co*-DMS respectively. Prior to pouring the mixture, the glass slides were plasma treated for 5 min (100W, 300s, 100 air) and hydrophobized with Tridecafluoro-1,1,2,2-tetrahydrooctyl-1-trichlorosilane for 30 min. Patterned stamps were produced by pouring the mixture over a Si master template (4 µm stripe patterns) or onto the patterned 3D-mold fixed in between the glass slides. The samples were cured at 90 °C for 4h and at 110 °C for 16h.

Conventional polydimethylsiloxane (PDMS) stamp was prepared from Slygard 184 kit. Prepolymer-to-curing agent (10:1, w/w) were mixed, degassed, and cured at 110 °C for 16h.

Poly{N-[tris(hydroxymethyl)methyl]acrylamide} (*PTrisAAm*) *grafting from stamp-surface.* A monomer solution (4 ml) was prepared with TrisAAm (350 mg, 2 mmol) in Milli-Q water. The solution was filtered through Al_2O_3 column to remove inhibitor. For a targeted DP of 1000, S-(2-propanoic acid) O-ethyl xanthate (Xan, 0.2 mg, 0.0010 mmol) was added to the filtered solution (2 ml, 175 mg, 1 mmol). For DPs 500 and 1500, 0.4 mg (0.002 mmol) and 0.128 mg (0.00066 mmol) Xan were used respectively. A clean stamp was suspended in the solution using a clamp. The solution was illuminated with UV light (365nm, 4W) for 1h. The stamp was washed thoroughly with Milli-Q water and dried with air stream afterwards.

Covalent attachment of APTES to the surface grafted PTrisAAm (Inking). In an Eppendorf tube APTES (1.3 mg, 0.00587 mmol) was dissolved in MeOH (1.3 ml). Sodium hydroxide (NaOH, 0.00234 mg, 5.87×10^{-5} mmol) was added to the solution as a catalyst. A single ~ 1 cm^2 stamp was suspended in the solution for 3h at 60 °C for the reaction. Afterwards the stamp was washed with MeOH, and EtOH respectively. The washed stamp was dried under vacuum at 60 °C for 20 min.

Swelling test. The tests were carried out immersing the novel stamps as well as the conventional PDMS stamp in 5 ml Toluene. For this test a sample dimension of ~ 6 × 5 × 1 mm (l × w × t) was considered. The stamp material was soaked in toluene for 24h. The swollen sample was transferred into an Eppendorf tube (1.5 mL) in the presence of glass wool at the bottom. Excessive toluene was removed using a centrifuge from Eppendorf (*miniSpin*) with a low centrifugal force (162 × *g*). Relative centrifugal force (RCF) was calculated for a rotor radius, R (from center of rotor to sample) of 3 cm and an rpm, S of 2200 with the following equation (1).

$$RCF = 1.118 \times 10^{-5}\, RS^2 \quad (1)$$

With mass increase of the swollen stamp, after a quick removal of the excessive toluene, the relative swelling degree is determined. All the samples were dried afterwards in an oven at 60 °C for 5h. The values are recorded as an average of 3 independent tests. Errors are shown in standard deviation. Gel fraction (%), swelling degree (%), and weight loss (%) were calculated from the following equations (2), (3) & (4) respectively.

$$\frac{Dried\ weight}{Initial\ weight} * 100 \quad (2)$$

$$\frac{Swollen\ weight - Dried\ weight}{Swollen\ weight} * 100 \quad (3)$$

$$\frac{Initial\ weight - Dried\ weight}{Initial\ weight} * 100 \quad (4)$$

Printing substrate preparation. To prepare silica-gel modified glass substrate, the glass substrate was plasma treated (100w, 60s, 100 air) first, and then hydrophobized by applying chemical vapor deposition (CVD) of chlorotrimethylsilane for 20 min. The substrate is dip-coated with trimethylsilyl [-Si(CH_3)$_3$] modified SiO_2 sol, synthesized according to the literature procedure.[55] at a withdrawing rate 400 mm min^{-1} and an immersion rate of 200 mm min^{-1}. After dip-coating the substrate was dried at 100 °C and then plasma treated prior to printing (100W, 60s, 100 air). For printing on a silicon wafer, 1 cm^2 wafer was taken and washed with RCA cleaning agent (5:1:1, Mili-Q water: Hydrogen peroxide: Ammonium hydroxide solution (28 – 30% w/w basis

NH_3 solution)) at 80 °C for 20 min. The substrate was then washed with Mili-Q water and EtOH. Soft air stream was applied to dry the substrate. Both substrates were plasma treated (100W, 60s, 100 air) prior to printing.

Ink transfer to substrate. For XPS measurement, Inked stamp (APTES as ink) was kept in a closed container along with separate vials containing acetic acid (> 99%) and Mili-Q water for 2 min prior to printing. In order to confirm the ink transfer *via* XPS, plain inked stamp was laid onto Si wafer substrate in a closed chamber and pressed with a 100 g weight on top for 20 min. Additionally, printing on silica-gel modified glass was performed at 1 N force for 20 min. In this case, a bare stamp was washed by immersing in EtOH overnight and dried under vacuum (10 mbar) at 60 °C for 1h. Dried stamp was inked by drop-casting with Rhodamine 6G (R6G) from a 10 µg per 1 ml Mili-Q water and then incubated for 1h in the dark. Later, printing was carried out for 10 s. A PTrisAAm-grafted stamp (the stamp prior to grafting was washed and dried in a similar fashion) inked with APTES and then washed with MeOH and EtOH respectively. The washed stamp after drying at 60 °C for 1h was labelled with Rhodamine B isothiocyanate (RBITC) for fluorescence imaging by dipping in 10 µg ml^{-1} solution (dry DMF) and incubated for 1h in the dark. After rinsing with EtOH, printing was carried out for 20 min. Printing on smooth and rough sides of the Si wafer was done with a force of 1 N, and 2 N respectively for 20 min. Except the stamp inked with R6G by drop-casting, prior to all printing experiments the inked stamps were kept along with acetic acid (> 99%) and Mili-Q water (separate vials) for 2 min in a closed container.

Fluorescence Labelling of printed substrate. Printed Si wafer substrates were immersed in a solution of 1 µg mL^{-1} (EtOH) NHS-ester based Alexa555 dye for labelling. The substrates were incubated in the dark for 1h and then washed with EtOH thoroughly.

ASSOCIATED CONTENT

SUPPORTING INFORMATION

NMR spectra, SEC data, mechanical data, light and fluorescence microscopy images, AFM height images of samples are found in the supporting information.

AUTHOR INFORMATION

Corresponding Author

Martin Reifarth.

Chair of Polymer materials and Polymer Technologies, University of Potsdam, 14476, Potsdam.

Fraunhofer Institute of Applied Polymer research, 14476 Potsdam.

Email: martin.reifarth@uni-potsdam.de

Authors

Nazim Pallab.

Chair of Polymer materials and Polymer Technologies, University of Potsdam, 14476, Potsdam.

Fraunhofer Institute of Applied Polymer research, 14476 Potsdam.

Stefan Reinicke.

Fraunhofer Institute for Applied Polymer research, 14476 Potsdam.

Johannes Gurke.

Chair of Polymer materials and Polymer Technologies, University of Potsdam, 14476, Potsdam.

Rainer Rihm.

Fraunhofer Institute for Applied Polymer research, 14476 Potsdam.

Matthias Hartlieb.

Chair of Polymer materials and Polymer Technologies, University of Potsdam, 14476, Potsdam.

Fraunhofer Institute of Applied Polymer research, 14476 Potsdam.

Notes

The authors declare no competing financial interest.

Conflicts of interest

Authors declare no conflict of interest.

ACKNOWLEDGMENT

The authors thank Prof. Alexander Böker of the Fraunhofer Institute for Applied Polymer Research (IAP) in Potsdam for his support. N.P. and M.R. acknowledge the German research council (DFG) for financial support (project number 471323994). M.H. gratefully acknowledges funding from the DFG (Emmy-Noether-Program, project number 445804074). The authors acknowledge the company ZUMOLab GmbH (Wesseling, Germany), which manufactured the printing device "ZUMO-MCP (Micro Contact Printer)" that is used in this study. The authors gratefully acknowledge the co-workers of the NMR facility at the institute of chemistry, University of Potsdam, including Prof. Dr. Heiko Möller, Dr. Matthias Heydenreich, and Angela Krtitschka. Anne-Catherine Lehnen is acknowledged for measuring size-exclusion chromatography. Prof. Dr. Helmut Schlaad and Sascha Prentzel from the Institute of Chemistry (University of Potsdam) are gratefully acknowledged for providing the SEC facility to perform measurements. Monica Heigel and Nicole Fischer are acknowledged for mechanical characterization of the materials.

REFERENCES

[1] M. Mirazul Islam, V. Cėpla, C. He, J. Edin, T. Rakickas, K. Kobuch, Ž. Ruželė, W. Bruce Jackson, M. Rafat, C. P. Lohmann, R. Valiokas, M. Griffith, *Acta Biomater.,* 2015, **12**, 70.

[2] C. D. Eichinger, T. W. Hsiao, V. Hlady, *Langmuir,* **2012**, **28**, 2238.

[3] E. P. Yalcintas, K. B. Ozutemiz, T. Cetinkaya, L. Dalloro, C. Majidi, O. B. Ozdoganlar, *Adv. Funct. Mater.,* 2019, **29**, 1906551.

[4] D. Li, L. J. Guo, *Appl. Phys. Lett.,* 2006, **88**, 063513.

[5] B. Wang, B. Koo, L. Huang, H. G. Monbouquette, *Analyst,* 2018, **143**, 5008.

[6] S.-M. Tsai, T. Goshia, Y.-C. Chen, A. Kagiri, A. Sibal, M.-H. Chiu, A. Gadre, V. Tung, W.-C. Chin, *Colloids Surf. B.,* 2018, **170**, 219.

[7] Y. Xia, G. M. Whitesides, *Annu. Rev. Mater. Sci.,* 1998, **28**, 153.

[8] M. Geissler, H. Kind, P. Schmidt-Winkel, B. Michel, E. Delamarche, Langmuir, 2003, **19**, 6283.

[9] C. D. James, R. C. Davis, L. Kam, H. G. Craighead, M. Isaacson, J. N. Turner, W. Shain, Langmuir, 1998, **14**, 741.

[10] T. Kaufmann, B. J. Ravoo, Polym. Chem., 2010, **1**, 371.

[11] A. Kumar, G. M. Whitesides, Appl. Phys. Lett., 1993, **63**, 2002.

[12] N. L. Jeon, R. G. Nuzzo, Y. Xia, M. Mrksich, G. M. Whitesides, Langmuir, 1995, **11**, 3024.

[13] L. Yan, W. T. S. Huck, X.-M. Zhao, G. M. Whitesides, Langmuir, 1999, **15**, 1208.

[14] L. Yan, X.-M. Zhao, G. M. Whitesides, J. Am. Chem. Soc., 1998, **120**, 6179.

[15] L. Zhai, D. W. Laird, R. D. McCullough, Langmuir, 2003, **19**, 6492.

[16] A. Bernard, J. P. Renault, B. Michel, H. R. Bosshard, E. Delamarche, Adv. Mater., 2000, **12**, 1067.

[17] A. Béduer, F. Seichepine, E. Flahaut, C. Vieu, Microelectron. Eng., 2012, **97**, 301.

[18] A. Perl, D. N. Reinhoudt, J. Huskens, Adv. Mater., 2009, **21**, 2257.

[19] W. Bao, D. Liang, M. Zhang, Y. Jiao, L. Wang, L. Cai, J. Li, Prog. Nat. Sci.: Mater., 2017, **27**, 669.

[20] M. J. Madou, Fundamentals of Microfabrication, CRC Press, 2018.

[21] T. Lohmüller, D. Aydin, M. Schwieder, C. Morhard, I. Louban, C. Pacholski, J. P. Spatz, Biointerphases, 2011, **6**, MR1.

[22] G. Liu, S. H. Petrosko, Z. Zheng, C. A. Mirkin, Chem. Rev., 2020, **120**, 6009.

[23] J. Hyun, S. J. Ahn, W. K. Lee, A. Chilkoti, S. Zauscher, Nano Lett., 2002, **2**, 1203.

[24] L. Stolz Roman, O. Inganäs, T. Granlund, T. Nyberg, M. Svensson, M. R. Andersson, J. C. Hummelen, *Adv. Mater.,* 2000, **12**, 189.

[25] T. F. Didar, M. Tabrizian, *Lab Chip,* **2012**, *12*, 4363.

[26] R. Kane, *Biomater.,* 1999, **20**, 2363.

[27] D. B. Weibel, A. Lee, M. Mayer, S. F. Brady, D. Bruzewicz, J. Yang, W. R. DiLuzio, J. Clardy, G. M. Whitesides, *Langmuir,* 2005, **21**, 6436.

[28] J. Li, L. Xu, S. Kim, A. A. Shestopalov, *J. Mater. Chem. C,* 2016, **4**, 4155.

[29] S. J. Clarson, J. A. Semlyen, *Siloxane Polymers*, Prentice Hall, Englewood Cliffs, N.J, 1993.

[30] K. J. Regehr, M. Domenech, J. T. Koepsel, K. C. Carver, S. J. Ellison-Zelski, W. L. Murphy, L. A. Schuler, E. T. Alarid, D. J. Beebe, *Lab Chip,* 2009, **9**, 2132.

[31] S.-S. D. Carter, A.-R. Atif, S. Kadekar, I. Lanekoff, H. Engqvist, O. P. Varghese, M. Tenje, G. Mestres, *Organs-on-a-Chip,* 2020, **2**, 100004.

[32] J. N. Lee, C. Park, G. M. Whitesides, *Anal. Chem.,* 2003, **75**, 6544.

[33] X. Wang, M. Sperling, M. Reifarth, A. Böker, *Small,* 2020, **16**, 1906721.

[34] I. Böhm, A. Lampert, M. Buck, F. Eisert, M. Grunze, *Appl. Surf. Sci.,* 1999, **141**, 237.

[35] D. J. Graham, D. D. Price, B. D. Ratner, *Langmuir,* 2002, 18, 1518.

[36] J. C. Love, L. A. Estroff, J. K. Kriebel, R. G. Nuzzo, G. M. Whitesides, *Chem. Rev.,* 2005, **105**, 1103.

[37] Y. Xia, N. Venkateswaran, D. Qin, J. Tien, G. M. Whitesides, *Langmuir,* 1998, **14**, 363.

[38] Y. Xia, E. Kim, M. Mrksich, G. M. Whitesides, *Chem. Mater.,* 1996, **8**, 601.

[39] A. Carvalho, M. Geissler, H. Schmid, B. Michel, E. Delamarche, *Langmuir,* 2002, **18**, 2406.

[40] E. Blinka, K. Loeffler, Y. Hu, A. Gopal, K. Hoshino, K. Lin, X. Liu, M. Ferrari, J. X. J. Zhang, *Nanotechnology,* 2010, **21**, 415302.

[41] M. Zimmermann, D. Grigoriev, N. Puretskiy, A. Böker, *RSC Adv.,* 2018, **8**, 39241.

[42] D. John, M. Zimmermann, A. Böker, *Soft Matter,* 2018, **14**, 3057.

[43] M. I. Maksud, M. S.Yusof, M. Mahadi Abdul Jamil, *Int. J. Integr. Eng.,* 2014, **5**, 36.

[44] M. Sperling, M. Reifarth, R. Grobe, A. Böker, *Chem. Commun.,* 2019, **55**, 10104.

[45] P. Akarsu, R. Grobe, J. Nowaczyk, M. Hartlieb, S. Reinicke, A. Böker, M. Sperling, M. Reifarth, *ACS Appl. Polym. Mater.,* 2021, **3**, 2420.

[46] P. Akarsu, S. Reinicke, A. Lehnen, M. Bekir, A. Böker, M. Hartlieb, M. Reifarth, *Small,* 2023, 2301761.

[47] A.-C. Lehnen, J. Gurke, A. M. Bapolisi, M. Reifarth, M. Bekir, M. Hartlieb, *Chem. Sci.,* 2023, **14**, 593.

[48] M. Hartlieb, *Macromol. Rapid Commun.,* 2022, **43**, 2100514.

[49] A.-C. Lehnen, J. A. M. Kurki, M. Hartlieb, *Polym. Chem.,* 2022, **13**, 1537.

[50] W. Wang, Q. Zhang, *J. Colloid Interface Sci.,* 2012, **374**, 54.

[51] Z. Zheng, J. Ling, A. H. E. Müller, *Macromol. Rapid Commun.,* 2014, **35**, 234.

[52] L. Wang, U. S. Schubert, S. Hoeppener, *Chem. Soc. Rev.,* 2021, **50**, 6507.

[53] H. Li, J. Zhang, X. Zhou, G. Lu, Z. Yin, G. Li, T. Wu, F. Boey, S. S. Venkatraman, H. Zhang, *Langmuir,* 2010, **26**, 5603.

[54] H. Li, J. Zhang, X. Zhou, G. Lu, Z. Yin, G. Li, T. Wu, F. Boey, S. S. Venkatraman, H. Zhang, *Langmuir,* 2010, **26**, 5603.

[55] D. Goswami, S. K. Medda, G. De, *ACS Appl. Mater. Interfaces,* 2011, **3**, 3440.